

# Enhancement of Space Durability of Materials and External Components Through Surface Modification

Y. Gudimenko,\* R. Ng,<sup>†</sup> J. Kleiman,<sup>‡</sup> and Z. Iskanderova<sup>§</sup>  
*Integrity Testing Laboratory, Inc., Markham, Ontario L3R 2R7, Canada*

D. Milligan<sup>¶</sup>  
*MacDonald Detwiler Space and Advanced Robotics, Ltd., Brampton, Ontario L6S 4J3, Canada*  
and

R. C. Tennyson\*\* and P. C. Hughes<sup>††</sup>  
*University of Toronto, Toronto, Ontario M3H 5T6, Canada*

**Results of surface modification treatment to improve space durability of main space-related thin polymer films, a lacing tape, and several organic-based thermal-control paints by a patented Photosil™ process are presented. Results of ground-based testing in an oxygen plasma asher and in a fast atomic-oxygen beam facility imitating low-Earth-orbit environment are also discussed. Characterization data before and after testing that include functional properties measurement, surface analyses, and durability evaluation are presented, and the protective mechanisms for Photosil treatment are discussed. Some of the samples that were treated in the program are similar to those in the Materials on International Space Station Experiment–1, being exposed now on the International Space Station. A number of space components including lacing tape and some external painted components of the Mobile Servicing System of the International Space Station were treated by Photosil, and the results will be discussed briefly.**

## Introduction

POLYMERS and polymer matrix composites have become vital engineering materials for spacecraft design because of their light weight and excellent strength and the fact that they can be used in applications where other materials could not, such as flexible, thin thermal insulation blankets and flexible second surface mirrors. The rationale to use polymeric materials and composites is quite simple: they allow engineers to explore new applications and clearly offer a scope for weight savings. Specially selected organic-based paints, mostly black and white, are often used as optical and thermal-control coatings. Advanced polymer materials, composites, and paints have been used in spacecraft structures, payloads, thermal control components, and power subsystem applications. One of the limits to using polymers, polymer-based paints, and polymer matrix composites in low Earth orbit (LEO) is the effect of atomic-oxygen (AO) erosion. Unprotected polymeric materials exposed to the AO environment in space undergo accelerated erosion, limiting their long-term use capability. The erosion effects of AO on polymeric materials and the use of various oxide-based protective coatings on thin polymer films, with all of their advantages and drawbacks, particularly for long-term missions, have been widely published.<sup>1–7</sup>

The patented Photosil™ surface-modification technology<sup>8,9</sup> has been developed to provide an alternative solution to the severe problem of AO erosion of polymer-based materials and composites in low-Earth-orbiting spacecraft. The Photosil process is a surface-modification technology that substantially alters the surface struc-

ture and chemistry of a polymer, incorporating silicon-containing groups into the subsurface layer (i.e., up to 1  $\mu\text{m}$  in depth) of the polymer structure. The surface becomes a new material and attains new properties. In essence, the Photosil process is a three-stage surface treatment consisting of 1) photoactivation of the surface, 2) liquid-phase silylation, and 3) stabilization that allows effective modification of a wide variety of polymers and composite materials, from polyethylene to complex polyimides.<sup>7–9</sup> In silylation reaction, the reactive hydrogen atoms from the functional groups formed in the activation stage are replaced with silicon groups from the chemical silylation agent, used for polymer surface treatment, creating organo-silicon molecules derived from the original polymer. Thus, the Photosil process produces a Si-containing uniformly graded surface layer without an abrupt transition boundary, thereby resisting cracking and spallation caused by thermal and physical stresses. Under certain circumstances, the modified surface structure also has a unique self-healing capability. A key advantage of the Photosil process is that only a thin layer near the surface is modified, resulting in very little or no change to the bulk material properties.

It was shown before, and confirmed further in this study, that this surface-modification treatment can not only significantly reduce but even eliminate the AO erosion of polymer-based materials used in spacecraft applications. Based on mass loss measurements, the treated materials exhibited averaged erosion yield of  $\leq 10^{-26}$  g/atom under fast ( $\sim 1\text{--}5\text{-eV}$ ) atomic oxygen (FAO) beam exposure, that is, two orders of magnitude lower than most pristine polymer materials used presently for space applications. In many cases, full surface stabilization and protection was successfully achieved, as confirmed by scanning electron microscopy, showing unchanged surface morphology. Various versions of the Photosil treatment were applied to a variety of materials including: Kapton® polyimide, Mylar® polyethylene terephthalate, polyetheretherketone (PEEK), polyethylene, polyvinyl chloride, polyamide, graphite fiber reinforced PEEK, and epoxy composites,<sup>7,8</sup> and some work was done for polyurethane-based paints.<sup>10</sup> The technological process was optimized in this study first for a number of space paints and other space-related materials, including a lacing tape. This treatment was also applied to metal-based external space components, painted with the just-mentioned paints or their mixtures. It is shown that in many cases the process does not significantly affect the thermal-optical properties or mechanical properties of

Received 1 December 2002; revision received 27 June 2003; accepted for publication 8 August 2003. Copyright © 2003 by the authors. Published by the American Institute of Aeronautics and Astronautics, Inc., with permission. Copies of this paper may be made for personal or internal use, on condition that the copier pay the \$10.00 per-copy fee to the Copyright Clearance Center, Inc., 222 Rosewood Drive, Danvers, MA 01923; include the code 0022-4650/04 \$10.00 in correspondence with the CCC.

\*Division Head, Chemical Analysis Division, 80 Esna Park Dr., Units 7-9.

<sup>†</sup>R&D Engineer, Chemical Analysis Division, 80 Esna Park Dr., Units 7-9.

<sup>‡</sup>President, Integrity Testing Laboratory, Inc., 80 Esna Park Dr., Units 7-9.

<sup>§</sup>Division Head, Space Materials Division, 80 Esna Park Dr., Units 7-9.

<sup>¶</sup>Staff Materials Engineer, 9445 Airport Road.

\*\*Professor, Institute for Aerospace Studies, 4925 Dufferin Street.

<sup>††</sup>Professor, Institute for Aerospace Studies, 4925 Dufferin Street. Associate Fellow AIAA.

the treated materials, a critically important factor for many space applications.

## Experimental

A number of materials and structures were treated and tested in ground-based testing facilities in this program. Therefore, the experimental conditions for each group will be described separately. Experimental work for each material was accomplished in two major phases: screening and optimization. Mixed-level algorithm statistical experimental designs were implemented in both the screening and optimization phases.

### Surface Modification of Materials and External Space Components

#### *Surface Modification of Polymer-Based Space Materials*

Ten different types of polymer-based selected space materials used mostly for thermal control and for other spacecraft applications were selected and used for this study. These materials were treated by different versions of the Photosil surface-modification technology. The materials represent clear and metallized thin polymer films, such as Kapton H, Kapton HN, Mylar, and PEEK, in a wide thickness range, as well as Kapton E, one of the prime candidates for inflatable structures and the so-called Gossamer Spacecraft materials,<sup>11</sup> polymer-based lacing cord, and three Aeroglaze® paints, white A-276 and two black, flat Z306 and glossy Z302, often used for thermal control and other space applications (Table 1). For the paints, space-grade Al-alloy disks and space-grade titanium alloy and stainless-steel metal coupons that represent the core materials of space components were used as substrates. Aeroglaze specifications for painting and curing involved a layer of special primer prior to painting. The dry paint film thickness was  $\sim 25\text{--}38\text{ }\mu\text{m}$  for Z306,  $\sim 51\text{--}76\text{ }\mu\text{m}$  for A276, and  $\sim 35\text{--}42\text{ }\mu\text{m}$  for Z302.

Various versions of the Photosil technology, including the most recent improvements and optimization, have been used. The variable treatment parameters were the type (UV or UV and corona) and energy of material pretreatment and posttreatment, which affects mostly the surface activation and stabilization stages, the temperature and time of silylation, and the type and concentration of silylation agent. For every material, a special study was conducted to optimize the activation and stabilization surface treatment conditions and duration, using UV treatment, as in Refs. 7 and 8, or a corona discharge +UV, as well as to optimize the silylation conditions, both through temperature and the silylation solution variations. All treated materials underwent extended ground-based test-

ing, and some of them have been provided for flight testing in the Materials on International Space Station Experiment, currently being exposed to the space environment.<sup>12</sup>

#### *Surface Modification of External Space Components and Lacing Tape*

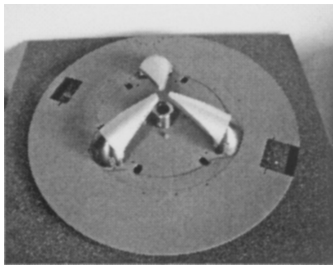
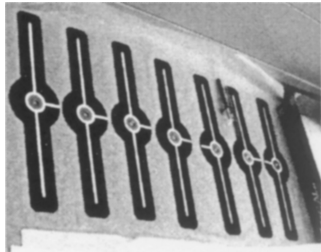
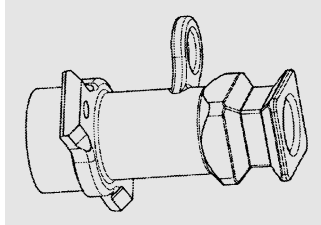
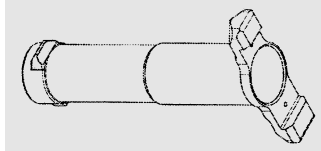
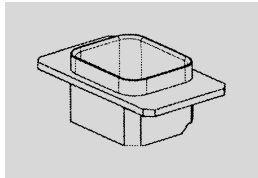

Various external International Space Station Mobile Servicing System space components, painted by the same Aeroglaze paints, and the lacing tape have been treated by Photosil for LEO space durability improvement. The description of painted external space metal components and tape that have been surface modified in the present work, their visual images, and treatment details are given in Table 2. In the treatment process of the painted surfaces of space components, the activation stage was conducted in a custom-made UV chamber under standard atmospheric conditions. This chamber is equipped with UV low-pressure quartz mercury vapor lamps that generate UV emission in the UV-C region with peaks at 254 and 185 nm. Four lamps, each 8.2 m long, are mounted in the chamber, with six more portable lamps, each 0.3 m in length, being used as necessary. UV treatment is used to create functional groups with active hydrogen atoms, such as hydroxyl (OH), in the surface region of the treated material. The activation process is a result of simultaneous excitation of polymer molecules and attack by molecular oxygen, as well as ozone, atomic oxygen, and singlet oxygen generated from molecular oxygen by the UV radiation. Maximum shelf life of the activated parts in this active state has been shown to be about 30 min; hence, the silylation stage was preferably performed immediately after activation.

The liquid-phase silylation was carried out in a specially designed and constructed chamber, which allows one to treat three-dimensional parts under low humidity ( $< 10\%$ ) and at temperatures between 30 and  $100^\circ\text{C}$ . Depending on the chemical structure of the surface to be treated, a number of different silylating agents, diffusion promoters, and solvents can be used to prepare the silylating solution. The solution can be applied by one of the commonly used painting techniques, such as dipping, brushing, spraying, depending on the size and dimensions of the parts. After the silylation at the prescribed temperature and time, the parts were rinsed with a solvent and dried under the silylation chamber conditions. The goal of the silylation process, as described in Refs. 8–10, is to replace the reactive hydrogen atoms from the functional groups formed in the activation stage with silicon groups from the silylating agent, creating the organo-silicon molecules derived from the original polymer.

**Table 1** Specification of materials selected for surface modification

Material	Chemical composition	Supplier	Sample characteristics
Kapton 100 H lot 92-02-1-1	Polyimide film	Sheldahl Corp.	1 mil
Polyester film Mylar type 500 D-1	Poly(ethylene terephthalate)	DuPont	5 mil
Kapton 50 E <sub>Ag</sub> Spec 3390	Polyimide film/silverized (for inflatables)	L'Garde, Inc.	0.5 mil
Kapton 50 E <sub>Au</sub> Spec 33902	Polyimide film/goldized (for inflatables)	L'Garde, Inc.	0.5 mil
PEEK film	Polyetheretherketone film	Westlake Plastics Co.	3 mil
Kapton 500 HN	Polyimide film	DuPont	5 mil
Kapton 500 H	Polyimide film	DuPont	5 mil
Lacing cord HT-30-TVS	Resin-impregnated Nomex fibers	MD Robotics	Lace (tape)
Black paint Aeroglaze Z302	Aromatic polyurethane- based thermal control paint (glossy)	Lord Corp.	Painted space- grade Al alloy disks, $d \approx 40\text{ }\mu\text{m}$
White paint Aeroglaze A276	Aliphatic polyurethane- based thermal control paint	Lord Corp.	Painted space- grade Al alloy disks, $d \approx 60\text{ }\mu\text{m}$
Black paint Aeroglaze Z306	Aromatic polyurethane- based thermal control paint (flat)	Lord Corp.	Painted space- grade Al alloy disks, $d \approx 30\text{ }\mu\text{m}$
Kapton E	Polyimide film	L'Garde, Inc.	0.5 mil

**Table 2** External space components protected by Photosil

Component	Description	Image
Grapple fixture (currently flying)	The grapple fixture is attached to a satellite or payload for the end effector of the remote-manipulator-system (RMS) robot arm to grasp and maneuver it. The grapple fixture is painted with polyurethane-based gray (Aeroglaze A276:Z306), black (Aeroglaze Z306), and white (Aeroglaze A276) paints. <sup>a</sup>	
Target plate and rod (currently flying)	Target plate/rod is used as a visual alignment aid to assist the operator in positioning the RMS robot arm end effector over the grapple shaft for capture. The visual cues of the target and rod are painted with black (Aeroglaze Z306) paint with white (Aeroglaze A276) markings.	
Upper housing (scheduled for 2005 launch)	Socket extension tool, external component of the Special Purpose Dexterous Manipulator Painted with gray paint (Aeroglaze A276:Z306)	
Lower housing (scheduled for 2005 launch)	Socket extension tool, external component of the Special Purpose Dexterous Manipulator Painted with gray paint (Aeroglaze A276:Z306)	
Baffle, camera (scheduled for 2005 launch)	Camera baffle built for the Special Purpose Dexterous Manipulator Painted with black paint (Aeroglaze Z306).	
Lacing tape (currently flying)	Aromatic polyamide (Nomex) flat-braided lacing cord impregnated with a synthetic resin. The braided fiber lacing tape is suitable for use with electrical wire harness assemblies.	

<sup>a</sup>Aeroglaze Z306 is a flat black absorptive paint, which consists of fumed silica and carbon black pigments in a polyurethane binder. Aeroglaze A276 is a white reflective paint made from titanium-dioxide pigment in a polyurethane binder. Gray polyurethane-based paint is a mixture of the Z306 and A276.

Stabilization of the silylated surface is required for converting the organo-silicon surface layer to a more oxidation resistant, oxidatively stable graded silicone-containing structure. The same setup as for photoactivation was used for stabilization of the silylated space components, and in every case the optimized conditions and duration for both activation and stabilization have been found.

A resin impregnated aromatic polyamide (Nomex<sup>®</sup>) fiber flat-braided lacing tape, suitable for spacecraft wire assemblies, was treated in a continuous feed Photosil process (Fig. 1). In this setup, the lace was continuously fed over a number of rollers mounted along the three-stage process. The photoactivation stage of the lace was conducted in an UV/ozone chamber system, and the activa-

tion conditions and duration have been optimized experimentally. Following activation, the lace was fed through a cylindrical aluminum vessel, where the liquid phase silylation stage took place. The vessel, filled with the silylating solution, was heated using a heating tape, wrapped around it. The controlled heating maintained the liquid bath inside the vessel at a prescribed temperature, which was found to be the most effective condition for the lace silylation process. After exiting the silylation bath, the lace was rinsed in a solvent bath and air dried before being rolled onto a take-up spool. The lace was fed through the system at a speed of approximately 3 m/h. Following a complete activation and silylation run, the lace was reloaded onto the feed spool and carried once again through the

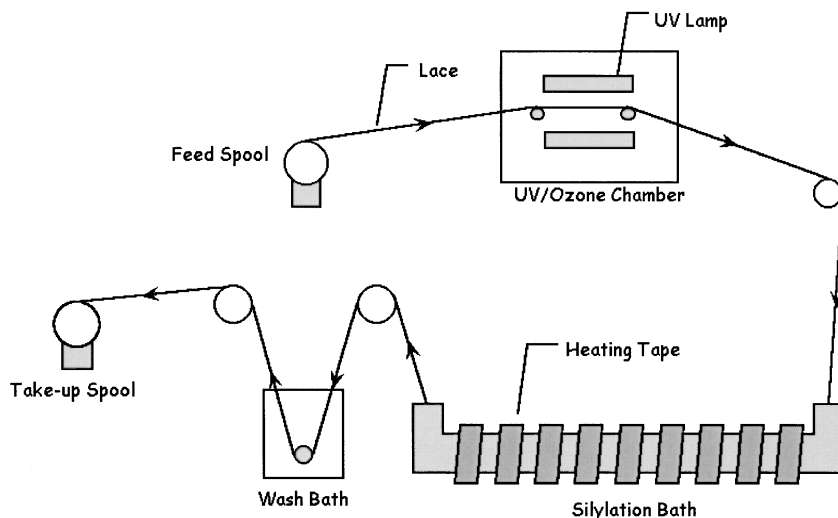


Fig. 1 Schematic diagram of the continuous lace Photosil treatment facility.

UV/ozone system, where the silylated lace underwent stabilization at experimentally optimized conditions.

#### Oxygen Plasma and Fast Atomic Beam Testing

Samples of materials listed in Table 1 and the specially prepared testing coupons representing the painted space components materials were tested in two different ground-based AO sources. An oxygen plasma asher and a recently upgraded fast atomic oxygen beam facility were used to test the samples before and after Photosil treatment, to determine the effectiveness of the AO protection. Plasma testing provides, in a comparatively easy way, the ability to create high-AO effective fluence exposures, but with thermal energy AO and other plasma species, and uncontrolled VUV radiation.<sup>13–15</sup> FAO beam testing more closely resembles the real LEO environmental conditions. It was shown many times in our ground-based studies that the oxygen plasma asher testing seems to be too harsh an environment for testing advanced self-protecting or surface modified polymeric and polymer-based materials.<sup>13–15</sup> Therefore, FAO beam testing is specifically required for ground-based testing and durability evaluation of those types of materials.

Plasma exposure tests were conducted in a low-temperature, inductively coupled radio frequency plasma asher. The asher operated at 13.56 MHz with the following settings: rf power  $\sim 200$  W, oxygen pressure  $\sim 100$  mtorr  $\pm 5\%$ , oxygen input  $\sim 100$  sccm  $\pm 5\%$ , and minimum average equivalent fluence  $\sim 1.9 \times 10^{20}$  atoms/cm<sup>2</sup>. The test and witness samples were placed in a holder and positioned in the middle of the 8-liter asher reactor. All samples were preconditioned in the plasma facility under vacuum for  $\sim 24$ –48 h for outgassing. The samples were exposed to the plasma for a minimum period of 5 h, which is equivalent to a total effective fluence of about  $1.9 \times 10^{20}$  atoms/cm<sup>2</sup>, as established from the mass loss for a control Kapton 500 HN sample ( $\sim 820$   $\mu\text{g}/\text{cm}^2$ ). Mass loss of the surface-modified samples was also measured by an electronic microbalance after the same time of plasma exposure.

FAO beam exposure tests were conducted in the recently modernized University of Toronto Institute for Aerospace Studies/Integrity Testing Laboratory Space Simulator similar to that described in Refs. 7–10. Each sample was placed in a holder that oriented the sample at 45 deg to the trajectory of the FAO beam. The samples were exposed to FAO with an energy  $\sim 3.0$  eV at an average flux of  $1 \times 10^{16}$  atoms/cm<sup>2</sup>  $\cdot$  s for a minimum period of 8–10 h and were held at a constant temperature for the duration of the test. More details on the FAO system can be found in Refs. 2 and 7. Similar control sets of samples were placed in the same chamber for the duration of the test outside the FAO beam. The mass loss of each of these samples was subtracted from the mass loss of the matching FAO-exposed specimen to account for mass loss caused by outgassing. If

no measurable mass loss occurs on the treated materials after FAO exposure, the estimated erosion yield cited for those materials represents the lower limit of mass loss, which could be measured by an electronic microbalance. In other words, when no mass loss can be measured within the accuracy of the equipment used the erosion yield associated with the resolution of the equipment is cited.

#### Surface Analysis and Characterization

To evaluate the changes in composition, structure, surface morphology, and functional characteristics, a number of complementary surface analysis and characterization methods have been used. The methods include X-ray photoelectron spectroscopy (XPS) and scanning electron microscopy combined with energy dispersive spectroscopy (SEM/EDS), with SEM employed in various modes.

For the treated external space components, described in Table 2, the major purpose of the applied paints was to improve the visual appearance and create the required color contrasts. In general, however, all thin polymer film materials and space paints of this program are mostly used as thermal control materials for space applications.<sup>16</sup> Therefore, the influence of the Photosil treatment on the major thermal-optical characteristics, solar absorptance  $\alpha$  and thermal emittance  $\epsilon$ , has been also analyzed.

Solar absorptance of the pristine, silylated, and silylated/FAO-treated materials has been measured using a spectrophotometer (Beckman Instruments, Model DK-2A) equipped with an integrating sphere. The solar absorptance in UV, visible, and near infrared (IR) ranges of the spectrum, covering the range 200–2450 nm was measured, and the final value was defined in accordance with the ASTM-E903 specification.<sup>17</sup> Thermal emittance of the same samples was measured in accordance with the ASTM-E408 specification,<sup>18</sup> using an infrared reflectometer manufactured by Gier Dunkle Instruments, Model DB100.

XPS analysis was carried out using a modified SSL SSX-100 x-ray photoelectron spectrometer. Survey scans of all samples were obtained using a 600- $\mu\text{m}$  x-ray spot size and 150-eV pass energy. The samples were analysed under a nickel grid to minimize peak distortion caused by charging effects.

SEM studies of all samples were performed on a Jeol JSM-T300 model microscope. The surfaces of the polymer samples were coated with a thin layer of carbon to prevent charging. An EDS x-ray microanalysis system URSA, manufactured by Mektech, was used for elemental analysis in some cases.

## Results and Discussion

#### Thin Polymer Films, Polyamide Fiber Lacing Tape, and Paint Samples

The results of oxygen plasma testing of space-related thin-film polymeric materials, lacing tape, and paint samples and coupons are



**Table 3 Process identification for Photosil treatment and oxygen plasma testing results**

Material	Chemical composition	Photosil process ID	Averaged relative erosion rate
Kapton H 1 mil lot 92-02-1-1	Polyimide film	Kapton H (C) <sup>a</sup>	≤0.16
Mylar polyester Mylar type 500D-1	Poly(ethylene-terephthalate)	Mylar (C)	≤0.25
Kapton E <sub>Ag</sub> spec 3390	Kapton 50E/silverized	Kapton Ag (C)	≤0.16
Kapton E <sub>Au</sub> spec 33902	Kapton 50E/goldized	Kapton Au (C)	≤0.16
PEEK natural film	Polyetheretherketone	PEEK (C)	≤0.25
Kapton 500 HN	Polyimide film	Kapton 500 HN (C)	≤0.14
Kapton 500 HN	Polyimide film	Kapton 500 HN	≤0.16
Kapton 500 H	Polyimide film	Kapton 500 H (C)	≤0.14
Kapton 500 H	Polyimide film	Kapton 500 H	≤0.16
Kapton 50 E	Polyimide film	Kapton E (C)	≤0.16
Lacing cord	Braided fibers, synthetic resin	Lacing tape	n/a
Black paint	Aromatic polyurethane-based paint	Black paint	≤0.1
Aeroglaze Z302			
White paint	Aliphatic polyurethane-based paint	White paint	≤0.1
Aeroglaze A276			
Black paint	Aromatic polyurethane-based paint	Black paint	≤0.1
Aeroglaze Z306			
Kapton 500 HN	Polyimide film	Pristine	1.00

<sup>a</sup>(C) is used to identify corona pretreatment.

presented in Table 3. The averaged erosion rate, which is the mass loss of the treated material specimen, averaged by plasma testing time, and relative to the mass loss of a Kapton 500HN witness, used as a standard, is presented for every material for different variants of the treatment process. To normalize the averaged erosion rates in the plasma facility,<sup>19</sup> the rate of erosion (by mass loss) for untreated Kapton 500HN was set to 1.0.

Some mass loss (mass change) can occur under AO exposure not only by erosion of the surface-modified samples (if any), but also because of additional oxidative surface conversion to fully stabilized protective oxide(s)-based “skin” during final stabilization, with competitive processes of volatiles release and oxygen uptake. The mass loss and the calculated average relative erosion rate given in such cases are just semiquantitative indications of the improved durability in an AO environment and require complementary SEM and other studies. In a preliminary study, all of the pristine materials used in this program demonstrated an oxygen plasma asher testing erosion rate quite close to Kapton 500 HN, and so it is clear that a reduction of plasma erosion rate by at least an order of magnitude (Table 3) was achieved for all of the treated materials.

The results of mass loss for all tested materials under the FAO beam are presented in Table 4. As can be seen from these results, the mass loss for the treated polymer films and lace was strongly reduced, being almost negligible for the metallized Kapton E and the lace, and with no measurable mass loss for the treated paints. The averaged erosion rate was not calculated because for surface-modified materials it is very difficult to distinguish between mass changes caused by the surface conversion processes at the surface during FAO exposure and the mass loss caused by erosion by FAO beam, if any. The conversion process is nonlinear, as determined by the measurements of the kinetics of mass loss of the modified polymer-based organic materials under FAO exposure.<sup>8–10</sup> It is practically impossible to distinguish the mass loss caused by reduced erosion and some mass loss (or mass change) caused by conversion process, that is, final stabilization of the treated samples that occur under the FAO beam. The final conclusion about durability improvement requires SEM studies at high magnification for evaluation of any change of surface morphology (see the following SEM results).

As just mentioned XPS surface analysis was used to characterize and verify the surface modification of the thin polymer films, lacing tape, and all paints used in this program. The results for films and lace are presented in Tables 5 and 6. For all Photosil-treated thin polymer films, the carbon content on the treated thin subsurface layer was significantly reduced, while the oxygen amount increased,

**Table 4 Results of FAO testing for materials treated by Photosil technology**

Material	Treatment	Mass loss after FAO exposure, $\mu\text{g}/\text{cm}^2$
Kapton 500 HN	Pristine (witness)	660
Kapton 500 HN	Silylated	60
Kapton 500 H	Pristine	650
Kapton 500 H (C)	Silylated	70
PEEK	Pristine	570
PEEK	Silylated	+50
Mylar	Pristine	860
Mylar	Silylated	70
Kapton 50 E	Pristine	190
Kapton 50 E	Silylated	70
Kapton 50 E <sub>Ag</sub>	Pristine	340
Kapton 50 E <sub>Ag</sub>	Silylated	10
Kapton 50 E <sub>Au</sub>	Pristine	340
Kapton 50 E <sub>Au</sub>	Silylated	30
Kapton 500 HN	Pristine	720
Kapton 500 HN	Silylated	30
Kapton 500 HN (C)	Silylated	+50
White paint A276	Pristine	480
White paint A276	Silylated	0
Black paint Z302	Pristine	550
Black paint Z302	Silylated	0
Black paint Z306	Pristine	280
Black paint Z306	Silylated	0
Lacing cord	Pristine	200
Lacing cord	Silylated	20

and ~15–25 at.% of Si appeared at the surface (see Table 5). These compositions, based on previous results,<sup>7–10</sup> are clear indications of a successfully completed Photosil surface treatment. The XPS elemental composition analysis revealed that in the upper layer of the Photosil-treated lacing tape the fluorine content has dropped sharply and the contents of silicon and oxygen have increased significantly. As a result of the Photosil treatment, silicon content has increased dramatically up to 20 at.% while oxygen makes up 23 at.% of the surface content (Table 6). These data confirm the modification of the uppermost surface region of the lace.

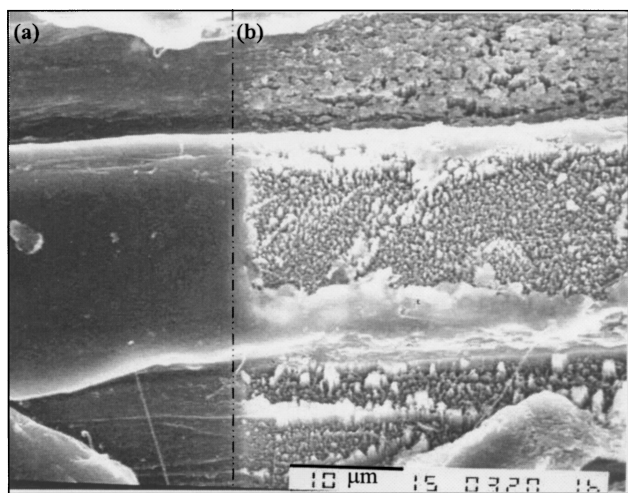
SEM at various magnifications was used to study the surface features of AO-exposed polymer films and lace and the erosion protection capability of the Photosil process for those materials. The SEM micrograph in Fig. 2 shows an untreated lace sample exposed to

**Table 5** Surface composition of pristine and silylated materials as determined by XPS

Materials/treatment	Elemental composition, at. %			
	C	O	N	Si
Kapton 500 HN pristine	76.62	16.64	6.33	0.36
Kapton 500 HN silylated	37.71	37.61	0.76	23.92
Kapton 500 HN silylated (C)	36.15	40.25	0.85	22.75
Kapton 500 H pristine	76.63	16.67	6.44	0.10
Kapton 500 H silylated	33.96	41.46	0.72	23.86
Kapton 500 H silylated (C)	39.71	37.48	0.82	22.00
Kapton 50 E pristine	77.31	16.09	6.28	0.24
Kapton 50 E silylated (C)	53.94	26.91	2.85	16.30
Kapton 50 E Ag pristine	77.31	16.09	6.28	0.24
Kapton 50 E Ag silylated (C)	45.23	30.12	0.79	23.86
Kapton 50 E Au pristine	77.47	15.99	6.22	0.24
Kapton 50 E Au silylated (C)	54.30	27.54	2.91	15.26
Mylar 500-1 pristine	73.13	26.62	0.00	0.07
Mylar 500-1 silylated (C)	36.85	39.22	0.47	23.46
PEEK pristine	81.45	15.89	0.00	2.56
PEEK silylated (C)	42.11	35.91	0.78	21.20
Kapton 100 H (1 mil, Sheldahl) pristine	77.65	15.65	6.53	0.10
Kapton 100 H (1 mil, Sheldahl) silylated	50.10	32.59	2.46	14.85

**Table 6** Surface composition of lace material (at. %) as determined by XPS

Specimen	Treatment	XPS chemical content, at. %				
		C	O	Si	N	F
Lacing tape	Control (untreated)	52.50	13.86	2.01	0.87	30.76
	Photosil	43.70	23.34	20.39	0.05	12.52

**Fig. 2** SEM micrograph of oxygen plasma exposed untreated lacing tape (effective fluence  $\sim 2.0 \times 10^{20}$  atoms/cm<sup>2</sup>) with magnification 2000 $\times$ : a) masked section and b) exposed section.

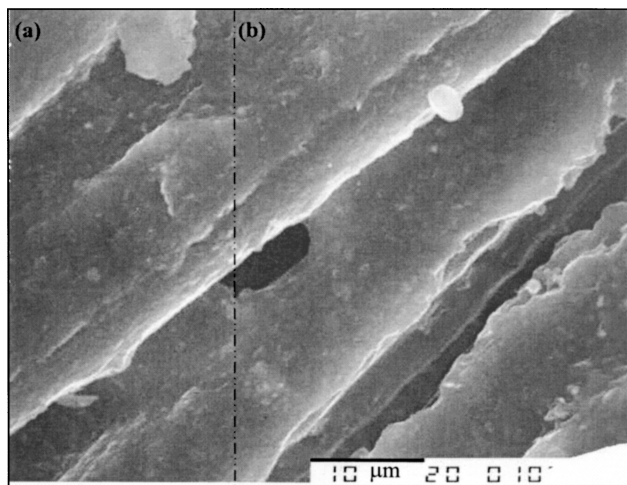
oxygen plasma for a total effective fluence of  $2.0 \times 10^{20}$  atoms/cm<sup>2</sup>, estimated from the mass loss of a control Kapton HN specimen that was exposed to the environment along with the tested lace. The left section that represents the untreated lace masked from AO shows no change in surface morphology, as expected; by contrast, the exposed area (right section) shows the typical highly eroded surface texture and the development of surface pores.

The Photosil-treated lace in Fig. 3 exhibits no visual features after exposure to oxygen plasma. For comparison purposes, the left section of the Photosil-treated lace was also masked from plasma, and the right section was exposed to plasma. No change in surface morphology was evident between these two sections, as noted in the SEM micrograph (Fig. 3). These visual results have demonstrated the protection effectiveness of the Photosil process. Similar results have been obtained after FAO beam testing.

**Table 7** Erosion yield<sup>a</sup> of polyurethane-based paints used on external space components

Material	Treatment	Erosion yield, g/atom	
		Plasma asher	Fast AO beam
Black paint	Control (untreated)	$8.90E-24$	$0.62E-24$
	Photosil	$0.60E-24$	$0.06E-24$
White paint	Control (untreated)	$7.92E-24$	$0.51E-24$
	Photosil	$0.25E-24$	$0.003E-24$
Gray paint	Control (untreated)	$4.69E-24$	$1.00E-24$
	Photosil	$0.41E-24$	$0.07E-24$
Black paint	Control (untreated)	$7.6E-24$	$0.52E-24$
	Photosil	$0.5E-24$	$0.05E-24$

<sup>a</sup>Values are strictly used as a means of comparison of averaged mass loss between untreated and Photosil-treated samples (see text).

**Fig. 3** SEM micrograph of oxygen plasma exposed Photosil-treated lacing tape (effective fluence  $\sim 2.0 \times 10^{20}$  atoms/cm<sup>2</sup>) with magnification 2000 $\times$ : a) masked section and b) exposed section.

#### Polyurethane-Based Paints for Painted External Space Components

Table 7 summarizes the average erosion yields, averaged by mass loss and time of exposure, for untreated and Photosil-treated paints, following both methods of ground-based accelerated AO exposure. These relative values represent the upper limits of these values and are used only for comparison because as already mentioned, for the treated paints some mass loss might be caused not by erosion, but by surface conversion under the AO fluxes. Photosil-treated paints

demonstrated those erosion yields upper limits about 1–2 orders of magnitude lower than the erosion yields of their respective untreated samples in both the plasma asher and FAO beam tests. These results demonstrated the AO erosion resistance of Photosil-treated paints and confirmed the successful surface modification of the painted space components.

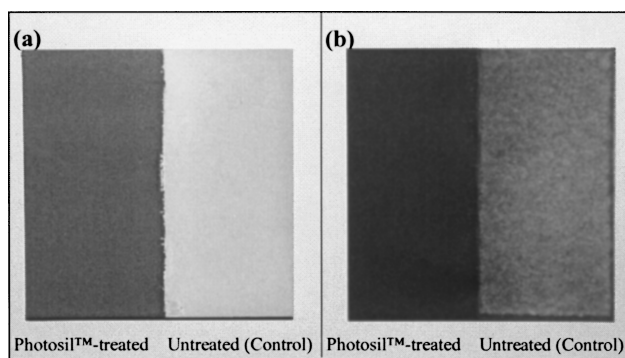
The surface chemical compositions, in relative atomic percentage, for control (pristine) and Photosil-treated paints were obtained from the XPS analysis. The results are shown in Table 8. Note that only survey scans for the elements of interest (C, O, Si, and N) were conducted. The XPS data indicate that considerable change has occurred in the Photosil-treated surface. The comparison between the control and treated paint samples shows the reduction of the carbon content and verifies the incorporation of silicon and oxygen into the surface region of the original paint material. These results again confirm the modification of the subsurface region of the polyurethane-based paints.

To effectively demonstrate the detrimental effect of AO exposure and the protective effectiveness of Photosil, an experiment was conducted where one-half of a painted coupon (left half) was treated by the Photosil process and the other half was left untreated. Photographs of gray (A276:Z306) and black painted coupons after 6- and 12-h oxygen plasma exposures are shown in Figs. 4 and 5, re-

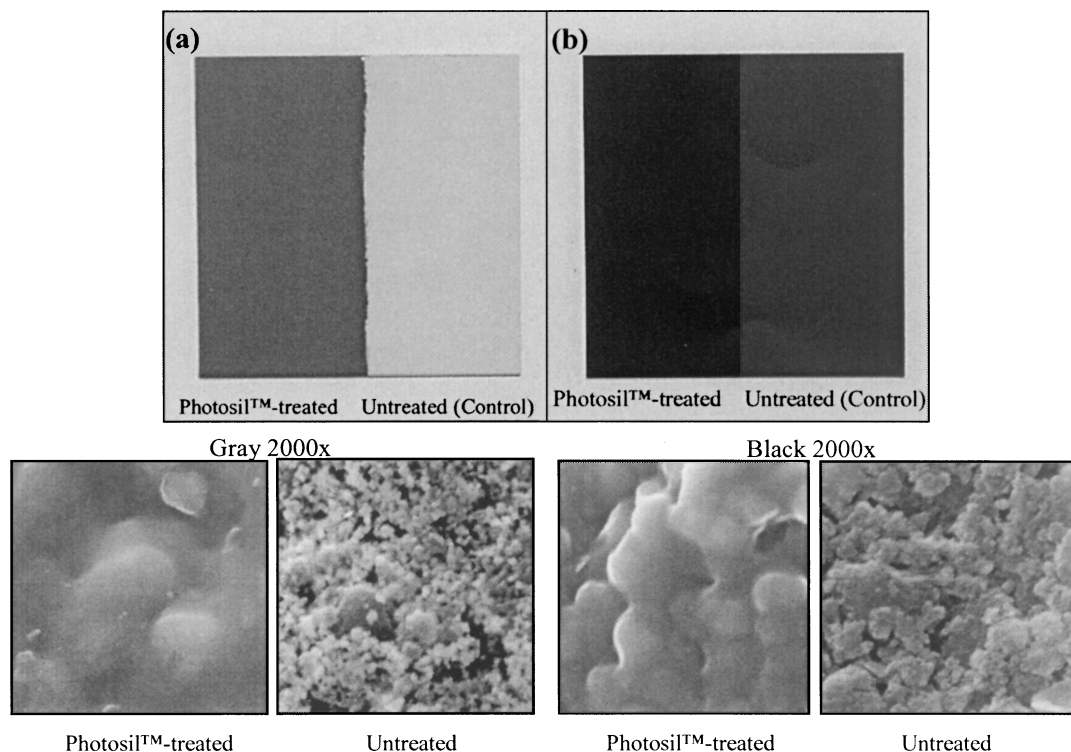
spectively. Visual results indicate the untreated half of the gray paint specimen exhibited considerable surface erosion after 6-h plasma exposure (effective fluence  $\sim 2.4 \times 10^{20}$  atoms/cm<sup>2</sup>) while the protected half was not eroded. The erosion was detected by visual observations of surface appearance and color change. The visual inspection also revealed that the AO eroded the polyurethane resin portion of the paint, leaving behind the pigments. The untreated gray surface attained a white powdery appearance (Fig. 4a). The loosely bounded white fine powders on the paint surface are the exposed titanium-dioxide pigments. The untreated black paint developed into a porous and powdery dark-gray surface (Fig. 4b). After the 12-h plasma exposure (effective fluence  $\sim 4.3 \times 10^{20}$  atoms/cm<sup>2</sup>), the Photosil-treated half remained almost intact with minor color fading. However, the untreated half was completely eroded, in particular the black (Z306) paint eroded to the point of exposing the primer (yellow) (Fig. 5b). The black paint, which consists of carbon black in polyurethane binder, was significantly eroded because of the reactive nature of AO to both carbon pigment and polyurethane. The gray (A276:Z306) paint, which contains polyurethane resin, titanium dioxide, and carbon pigments, also was severely eroded.

**Table 8** Surface composition of polyurethane-based paints (at%) measured using XPS

Specimen	Treatment	XPS chemical content, at. %			
		C	O	Si	N
Gray paint (A276:Z306)	Control (untreated)	75.07	20.47	1.44	3.02
	Photosil	40.29	32.92	26.33	0.46
Black paint Z306 (flat)	Control (untreated)	70.38	27.77	0.35	1.50
	Photosil	41.32	32.23	26.17	0.28
White paint A276	Control (untreated)	75.78	19.47	0.56	4.20
	Photosil	40.77	31.15	27.45	0.63
Black paint Z302 (glossy)	Control (untreated)	72.33	23.45	1.62	2.6
	Photosil	30.64	42.85	26.15	0.36



**Fig. 5** Painted test coupons exposed for 12 h to oxygen plasma (effective fluence  $\sim 4.3 \times 10^{20}$  atoms/cm<sup>2</sup>): a) gray (mixture of Z306 and A276) paint and b) black (Z306) paint.

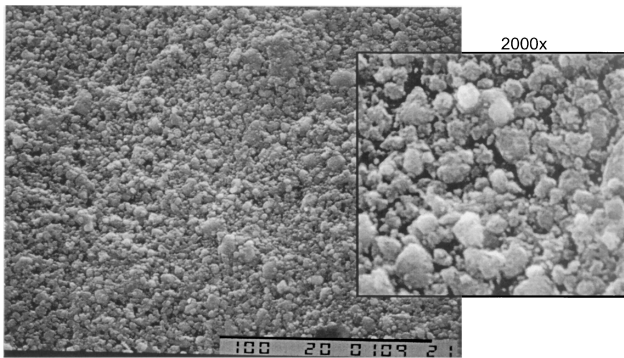
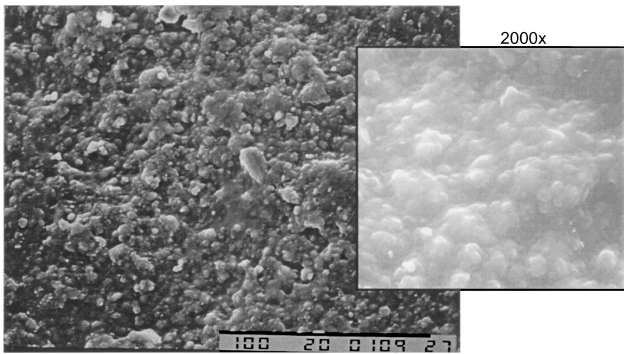


**Fig. 4** Painted test coupons exposed to oxygen plasma for 6-h (effective fluence  $\sim 2.4 \times 10^{20}$  atoms/cm<sup>2</sup>): a) gray (mixture of Z306 and A276) paint and b) black (Z306) paint.

**Table 9** Thermal-optical properties of pristine, silylated, and silylated/FAO-tested thin space-related polymer films

Materials/treatment	Thermal optical properties		
	$\alpha$	$\varepsilon$	$\alpha/\varepsilon$
Kapton E <sub>Ag</sub> /pristine	0.186	0.413	0.45
Kapton E <sub>Ag</sub> /silylated (C) <sup>a</sup>	0.207	0.425	0.48
Kapton E <sub>Ag</sub> /silylated (C)/FAO	0.212	0.428	0.49
Kapton E <sub>Au</sub> /pristine	0.488	0.424	1.15
Kapton E <sub>Au</sub> /silylated (C)	0.495	0.440	1.13
Kapton E <sub>Au</sub> /silylated (C)/FAO	0.483	0.430	1.12
Kapton H (1 mil, Sheldahl) pristine <sup>b</sup>	0.347	0.644	0.54
Kapton H (1 mil, Sheldahl)/silylated	0.351	0.647	0.54
Kapton H (1 mil, Sheldahl) silylated/FAO	0.352	0.651	0.54

<sup>a</sup>(C) indicates corona pretreated. <sup>b</sup>Measured with shiny Al foil backing.

**Fig. 6** SEM micrograph of untreated black (Z306) paint after FAO exposure (effective fluence  $\sim 3.6 \times 10^{20}$  atoms/cm<sup>2</sup>) with magnification 500 $\times$ .**Fig. 7** SEM micrograph of Photosil-treated black (Z306) paint after FAO exposure (effective fluence  $\sim 3.6 \times 10^{20}$  atoms/cm<sup>2</sup>) with magnification 500 $\times$ .

Both the resin and the carbon black were eroded away from the surface leaving behind the titanium-dioxide pigment particles. The stability of pigment particles is attributed to the AO resistance nature of titanium dioxide. The degradation effects of AO exposure on these paints have been widely published.<sup>1,5,6</sup>

In addition to the plasma asher exposure, FAO beam testing was conducted on the painted coupons. The SEM image in Fig. 6 clearly demonstrates the severe degradation effect of FAO on pristine black (Z306) paint. The polyurethane binder was eroded from the surface leaving the exposed loosely bound carbon black pigment. In contrast, no binder erosion was detected in the SEM micrograph of the FAO-exposed Photosil-treated paint (Fig. 7). Stability similar to that with FAO exposure was confirmed by SEM studies for the white (A276) and gray (A276:Z306) paints.

#### Thermal Optical Properties of Thin Films and Paints

The results of the measurements of the major thermal optical properties—the most important for thermal control applications—for some of the advanced thin polymer films and for all paints,

**Table 10** White, black, and gray Aeroglaze paints on space-grade Al-alloy or other space metal substrates, corresponding to external space components

Material/treatment	Thermal optical properties		
	$\alpha$	$\varepsilon$	$\alpha/\varepsilon$
Black paint Z302/pristine	0.962	0.824	1.16
Black paint Z302/silylated	0.973	0.850	1.15
Black paint Z302/silylated/FAO	0.942	0.835	1.14
White paint A276/pristine	0.170	0.880	0.19
White paint A276/silylated	0.172	0.876	0.19
White paint A276/silylated/FAO	0.173	0.878	0.19
Black paint Z306/pristine	0.971	0.912	1.06
Black paint Z306/silylated	0.983	0.911	1.07
Black paint Z306/silylated/FAO	0.959	0.899	1.07
Gray paint (A276:Z306)	0.879	0.882	1.00
Gray paint/silylated	0.885	0.892	0.99
Gray paint/silylated/FAO	0.887	0.894	0.99

corresponding to the space components, are presented in Tables 9 and 10. The data were collected on pristine, surface-modified, and modified/FAO tested materials.

It is evident from the results that for specially selected Photosil treatments the surface modification does not significantly affect the thermal-optical properties of the materials. The stabilization effect prevents them from being changed under FAO exposure in LEO-simulated ground-based testing. The ability to maintain the thermal-optical properties of the advanced polymer-based thermal control materials after the applied surface modification treatment and after the following FAO exposure is very important for various space applications.

## Conclusions

A surface-modification process Photosil was successfully applied to a number of thin polymer space-related films, polymer thermal control materials, painted surfaces of external spacecraft components, as well as to a polyamide fiber-based lacing tape. All treated materials were effectively protected from atomic oxygen erosion, as was confirmed in a series of ground-based tests. The surface chemistry of the treated materials was substantially altered, and the silicon content on the surface increased to the range of 15–25 at.%, depending on the material. The main thermal optical properties of the treated materials, such as the solar absorptance and the thermal emittance, did not change. The surface morphology of the treated materials remained unchanged, after ground-based testing in a fast-atomic-oxygen beam facility and oxygen plasma asher. The Photosil technology has proved to be a practical solution for protection of the polymer materials in LEO. Through incorporating of silicon-containing functional groups into the subsurface layer of the polymer structure, the surface modification creates unique stabilization and protection properties, so that the Photosil process can be used for polymer modification with potential application for long-term flights in the LEO space environment.

## Acknowledgments

The authors acknowledge B. A. Banks for encouraging discussions and support with the materials on International Space Station Experiment experiment and V. Farrel for providing the samples of space-grade aluminum-alloy substrates painted with the Aeroglaze white and black paints, as well as Rana Sodhi for x-ray photoelectron spectroscopy analysis.

## References

- Banks, B. A., "Atomic Oxygen," *LDEF Materials Data Analysis Workshop*, NASA CP 10046, 1990, pp. 191–217.
- Tennyson, R. C., "Atomic Oxygen Effects on Polymer-Based Materials," *Canadian Journal of Physics*, Vol. 69, No. 8, 9, 1991, pp. 1190–1208.
- Whittaker, A. F., Kamenetzky, R. R., Finckenor, M. M., and Norwood, J. K., "Atomic Oxygen Effects on LDEF Experiment AO171," *Proceedings of the Second LDEF Post-Retrieval Symposium*, NASA CP 3194, Pt. 3, edited by A. Levine, 1992, p. 1125.

<sup>4</sup>Golden, J. L., "Selected Results for LDEF Thermal Control Coatings," *Proceedings of the Second LDEF Post-Retrieval Symposium*, NASA CP 3194, Pt. 3, edited by A. Levine, 1992, p. 1099.

<sup>5</sup>Silverman, E. M., "Space Environmental Effects on Spacecraft: LEO Materials Selection Guide," NASA CR 4661, Pt. 1-2, Aug. 1995.

<sup>6</sup>Reddy, R., "Review: Effects of Low Earth Orbit Atomic Oxygen on Spacecraft Materials," *Journal of Materials Science*, Vol. 30, No. 2, 1995, pp. 281-307.

<sup>7</sup>Gudimenko, Y., Iskanderova, Z., Kleiman, J. I., Cool, G., Morison, D., and Tennyson, R., "Erosion Protection of Polymer Materials in Space," *Proceedings of the 7th International Symposium on Materials in a Space Environment*, ENSAE-SUPAERO, Toulouse, France, 1997, pp. 403-410.

<sup>8</sup>Gudimenko, Y., Kleiman, J. I., Iskanderova, Z. A., Tennyson, R. C., and Cool, G. R., U.S. Patent 5,948,484, issued 7 Sept. 1999.

<sup>9</sup>Kleiman, J. I., Iskanderova, Z. A., Gudimenko, Y. I., Morison, W. D., and Tennyson, R. C., "Polymers and Composites in the Low Earth Orbit Space Environment: Interaction and Protection," *Canadian Aeronautics and Space Journal*, Vol. 45, No. 2, 1999, pp. 148-160.

<sup>10</sup>Kleiman, J. I., Gudimenko, Y., Iskanderova, Z., Tennyson, R. C., and Morrison, W. D., "Modification of Thermal Control Paints by Photosil™ Technology," *Proceedings of the Fourth International Space Conference*, edited by R. C. Tennyson and J. Kleiman, Kluwer Academic, Norwell, MA, 2001, pp. 243-252.

<sup>11</sup>Jenkins, C., (ed), *Gossamer Spacecraft: Membrane and Inflatable Structures Technology for Space Applications*, AIAA, Reston, VA, 2001.

<sup>12</sup>"MISSE Master," NASA Langley Research Center, Hampton, VA,

URL: <http://www.MisSE.larc.nasa.gov/index.html> [cited 20 Aug. 2001].

<sup>13</sup>Whittaker, A. F., and Tang, B. Z., "Oxygen Plasma Environment: Its Effect on Polymers," *SAMPE Journal*, Vol. 30, No. 2, 1994, pp. 30-41.

<sup>14</sup>Townsend, J. A., and Park, G., "A Comparison of Atomic Oxygen Degradation in Low Earth Orbit and in a Plasma Etcher," *19th Space Simulation Conference*, NASA CP-3341, Jan. 1997, pp. 295-304.

<sup>15</sup>Dever, J., McCracken, C., and Bruckner, E., "RF Plasma Asher Vacuum Ultraviolet Radiation Characterization and Effects on Polymer Films," *Proceedings of the 6th International Conference "Protection of Materials and Structures from Space Environment"*, edited by J. Kleiman and Z. Iskanderova, Kluwer Academic, 2002, pp. 335-350.

<sup>16</sup>Gilmore, G. G., and Bello, M., *Satellites Thermal Control Handbook*, Aerospace Corp. Press, El Segundo, CA, 1994.

<sup>17</sup>"Test Method for Total Emittance of Surfaces Using Inspection-Meter Technique," Annual Book of ASTM Standards, E408, Vol. 15.03, American Society for Testing and Materials, Philadelphia, 1995.

<sup>18</sup>"Test Method for Solar Absorptance, Reflectance, and Transmittance of Materials Using Integrating Spheres," Annual Book of ASTM Standards, E903, Vol. 12.02, American Society for Testing and Materials, Philadelphia, 1995.

<sup>19</sup>Koontz, S. L., Albyn, K., and Leger, L. J., "Atomic Oxygen Testing with Thermal Atom Systems: A Critical Evaluation," *Journal of Spacecraft and Rockets*, Vol. 28, No. 3, 1991, pp. 315-323.

D. Edwards  
Associate Editor

## Analytical Mechanics of Space Systems

Hanspeter Schaub, ORION International Technologies and John L. Junkins, Texas A&M University



This book provides a comprehensive treatment of dynamics of space systems starting with the basic fundamentals. This single source contains topics ranging from basic kinematics and dynamics to more advanced celestial mechanics; yet all material is presented in a consistent manner. The reader is guided through the various derivations and proofs in a tutorial way. The use of "cookbook" formulas is avoided. Instead, the reader is led to understand the underlying principle of the involved equations and shown how to apply them to various dynamical systems.

The book is divided into two parts. Part I covers analytical treatment of topics such as basic dynamic principles up to advanced energy concept. Special attention is paid to the use of rotating reference frames that often occur in aerospace systems. Part II covers basic celestial mechanics treating the two-body problem, restricted three-body problem, gravity field modeling, perturbation methods, spacecraft formation flying, and orbit transfers.

A Matlab® kinematics toolbox provides routines which are developed in the rigid body kinematics chapter. A solutions manual is also available for professors. Matlab® is a registered trademark of The MathWorks, Inc.

### Contents:

Part I: Basic Mechanics • Particle Kinematics • Newtonian Mechanics • Rigid Body Kinematics • Eulerian Mechanics • Generalized Methods of Analytical Dynamics • Nonlinear Spacecraft Stability and Control • Part II: Celestial Mechanics • Classical Two-Body Problem • Restricted Three-Body Problem • Gravitational Potential Field Modeling • Perturbation Methods • Spacecraft Formation Flying • Orbit Transfers • Interplanetary Trajectories

AIAA Education Series  
2003, 600 pages, Mixed media  
ISBN: 1-56347-563-4  
List Price: \$105.95  
**AIAA Member Price: \$74.95**



American Institute of  
Aeronautics and Astronautics

Publications Customer Service, P.O. Box 960  
Herndon, VA 20172-0960  
Phone: 800/682-2422; 703/661-1595 • Fax: 703/661-1501  
E-mail: [warehouse@aiaa.org](mailto:warehouse@aiaa.org) • Web: [www.aiaa.org](http://www.aiaa.org)

03-0614